Available online at www.sciencedirect.com

ScienceDirect

Procedia Engineering 138 (2016) 19 – 29

Procedia Engineering

www.elsevier.com/locate/procedia

"SYMPHOS 2015", 3rd International Symposium on Innovation and Technology in the Phosphate Industry

Preliminary data of REE in Algerian phosphorites: a comparative study and paleo-redox insights

Rabah Kechiched[a-b*], Rabah Laouar[a], Olivier Bruguier[c], Sihem Laouar-Salmi[a], Ouafi Ameur-Zaimeche[b] & Atif Foufou[d]

[a] *Département de Géologie, Université Badji Mokhtar Annaba B.P.12, Annaba, 23000 Algérie*
[b] *Laboratoire des Réservoirs Souterrains: Pétroliers, Gaziers et Aquifères, Université Kasdi Merbah Ouargla, 30000 Algérie*
[c] *Géosciences Montpellier, Université de Montpellier, CNRS-UMR 5243, Place E. Bataillon, 34095 Montpellier cedex 5, France*
[d] *Faculté des Sciences de la Nature et de la Vie, Université Ziane Achour Djelfa, Algérie*

Abstract

This study deals with the preliminary data of rare earth elements (REE) obtained on northeastern Algerian phosphorites from the Tébessa region. These phosphorites are located in two different basins: the northern basin represented by Dj. El Kouif, Dj. Dyr and Tazbant showings and the southern basin with the giant Dj. Onk phosphate deposit. The host sedimentary formation is Late Paleocene to Early Eocene. Twenty-six (26) samples from the four (4) localities were collected and analyzed for their REE contents using the ICP-MS technique. Phosphates from the southern basin (Dj. Onk deposit) show ∑REE contents ranging from 174.41 and 906.39 ppm (average ∑REE = 623.01 ppm), while the northern phosphorites have lower ∑REE contents (from 125.45 to 472.44 ppm; average = 265.57 ppm). PAAS-normalized REE patterns and binary Box plot of $(Sm/Pr)_N$ vs $(Sm/Yb)_N$ show HREE enrichments for samples from the northern localities while most samples from the southern basin are HREE depleted. Normalized $(La/Yb)_N$ vs $(La/Sm)_N$ plot shows that $(La/Sm)_N$ ratios of all samples are similar to those of modern seawater (from 0.83 to 1.55). However, the $(La/Yb)_N$ ratios of the two basins are significantly higher (from 0.67 to 1.18), which indicates an early diagenesis. The Ce/Ce* vs Pr/Pr* diagram shows that the observed Ce anomaly was not affected by diagenesis and more likely represents a proxy for redox conditions. The obtained results substantiate that the northern phosphorites were formed in more oxic environment with more pronounced negative Ce anomalies, whereas the southern phosphorites have lower Ce anomalies. Northern phosphorites are different from those from the south probably because the northern basin was more connected to an open sea as did the Sra Ouartan basin in northern Tunisia. These results have also been confirmed by statistical method studies, such as factorial discriminate analysis.

* Corresponding author. Tel.: +213 661 214 544;
E-mail address: kechiched.ra@univ-ouargla.dz

Peer-review under responsibility of the Scientific Committee of SYMPHOS 2015
doi:10.1016/j.proeng.2016.02.048

Peer-review under responsibility of the Scientific Committee of SYMPHOS 2015

Keywords: Phosphorites; HREE; LREE; Ce anomaly; Tébessa.

1. Introduction

The geochemistry of rare earth elements (REE) in sedimentary phosphorites has been studied by many authors as it brings important insights in reconstructing paleo-depositional environments eg. [1-10]. Algerian phosphorites are located mainly in the Tébessa area (600 Km southeast of Algiers) (Fig. 1), and are part of many deposits and showings that outcrop in northern Africa. These phosphorites are hosted by Paleocene to Eocene marine formation. The present study focuses on phosphorites located in two different basins: (a) The northern basin comprises Djebel el Kouif, Djebel Dyr and Djebel Tazbant showings and (b) the southern basin consists of the giant Kef Essennoun phosphorite deposit of Djebel Onk region. A comparative study of the REE behavior in phosphorites from these basins is carried out in order to highlight paleo-redox environments in which these phosphorites were deposited.

Nomenclature

REE	Rare earth elements
HREE	Heavy rare earth elements
LREE	Light rare elements
Ce_{An}	Cerium anomaly
FDA	Factorial discriminate analysis

2. Presentation of studied areas and sampled outcrops

The investigated phosphorites are hosted by Late Paleocene to Early Eocene marine formations and are a result of a large period of phosphogenesis that occurred in the Tethys Ocean from North Africa to the Middle East [11-15]. Phosphogenesis occurred during this period in northeastern Algeria as a result of upwelling currents, and phosphatic material was deposited around Kessrine Island that was formed as emerged zone during the Paleocene-Eocene period. Three major basins were individualized: (1) the Sra Ouartan basin (northern basin); (2) the Meknassy-Mezzouna basin (eastern Tunisia basins); and (3) the Gafsa-Metlaoui-Onk basin (Southern basin). The most important deposits and phosphorites showings in Algeria are located in the eastern Saharan Atlas close to the Tunisian border and are distributed in two different basins: the northern basin (Dj. El Kouif; Dj. Dyr. and Tazbant showings) and the southern basin (Dj. Onk giant deposits) (Fig. 1).

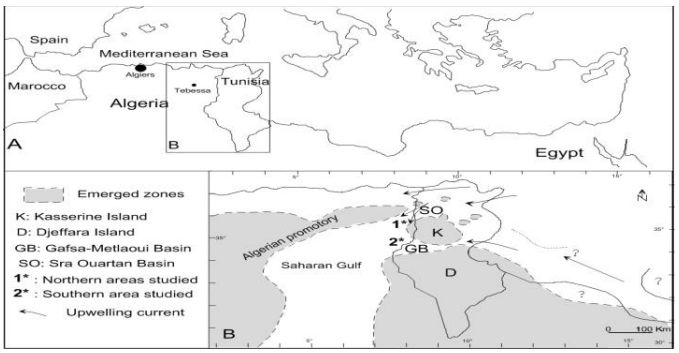

Fig. 1. (A) Geographic position of the studied areas. (B): Paleogeographic situation of the Algero-Tunisian phosphorites during the early Eocene with location of the investigated areas [16-21].

2.1. Northern basin

The sedimentary sequences of the northern basin were studied by many authors eg. [22-27]. The outcrops are represented by a series of Early Cretaceous (Albian) to Miocene formations that are partly overlain by Quaternary continental formations. NE-SW-oriented Triassic evapaoritic diapirs intrude these series and are brought up to the surface under the Atlasic (Eocene) tectonic events. Phosphorites are hosted within Tertiary formations (Paleocene-Early Eocene). Carbonaceous formations are contemporaneous to phosphorite mineralization and indicate sedimentation in an open marine environment. The phosphorites are glauconite-bearing, fine-grained, hard and compact rocks, interbedded with thin layers of marls [28]. Below is a brief description of phosphorite outcrops (Fig. 2):

- Djebel Dyr consists of a perched syncline located nearby Tebessa city. It shows tabular structure that was affected by a number of E-W faults. The phosphorites occur as thin layers (from 10 cm to 50 cm thick) between marls and dolomites at the bottom and cherty limestones on top.
- Djebel El Kouif is located at about 20 km northeast of Tébessa city. The sedimentary outcrops occur as tabular structures and range in age from Late Paleocene to Early Lutetian. The lithology is dominated by limestones and marls and shows five phosphorite interlayers [28]. Their thickness range from 10 cm to 60 cm.
- Tazbant prospect is located at 10 km southeast of Tébessa city. The Paleocene-Eocene formation which overlays the Maastrichtian [29] consists of marls alternating with limestone and cherty limestone and shows thin (20 cm) levels of phosphorites.

2.2. Southern basin

The Gafsa-Metlaoui-Onk basin (Fig. 1) is characterized by a subsidence with a major control of NW-SE and W-E faults [31]. Many authors suggest that sedimentation involved restricted water exchanges with the eastern open sea at that period [16-17,28,30]. Dejbel Onk mining district belongs to the Gafsa-Metlaoui-Onk basin, and phosphorite mineralization is distributed into five sectors: Kef Essennoun, Djemi Djema, Bled El Hadba, Northern Djebel Onk and Oued Betita [31-35]. Kef Essennoun is taken as an example and was sampled for this study. The regional geology was studied in detail by Visse [31] and later by Prian and Cortiel [36]. The lithologies of Djebel Onk region are composed of a succession of about 500 m thick sedimentary layers that were deposited during the Upper Cretaceous (Maestrichtian) to Middle Eocene (Lutetian). The latter is partly covered by Quaternary continental clastic sediments (sandstones and clays). The Kef Essennoun deposit is characterized by a thick layer (~ 35 m) of Upper Thanetian phosphorites (Fig. 2) which is, itself, divided into 3 sub-layers known in all Djebel Onk district according to the P_2O5 and MgO contents [36]. From the bottom to the top, these sub-layers are:

- *The basal sub-layer*: It consists of about 2 m thick alternation of marl, phosphorites and dolomite. Phosphorites show relatively low P_2O_5 content (from 13 to 15 %) and high MgO content (8 to 10 %). Heterogeneous phosphorite grains are cemented by marl and clay matrix.
- *The main sub-layer*: It has a thickness of 25 to 30 m and is mined for phosphorites. It is characterized by high P_2O_5 content (24 to 28 %) and low MgO content (less than 4 %). Homogeneous phosphorite particles are cemented by clay or carbonaceous cement.
- *The Upper sub-layer*: It is composed of a phosphatic dolomite layer with relatively low P_2O_5 content (14 to 18 %) and MgO high content (6 to 11 %). This sub-layer is also characterized by a high SiO_2 content ranging from 1 to 6 %. Phosphorites particles are heterogeneously grained.

3. Analytical techniques

Twenty-six bulk phosphorite samples were collected from four different deposits in the northern and southern basins. Three (3) localities belong to the northern basin: Dj. El Kouif (8 samples), Dj. Dyr (9 samples), Dj. Tazbant

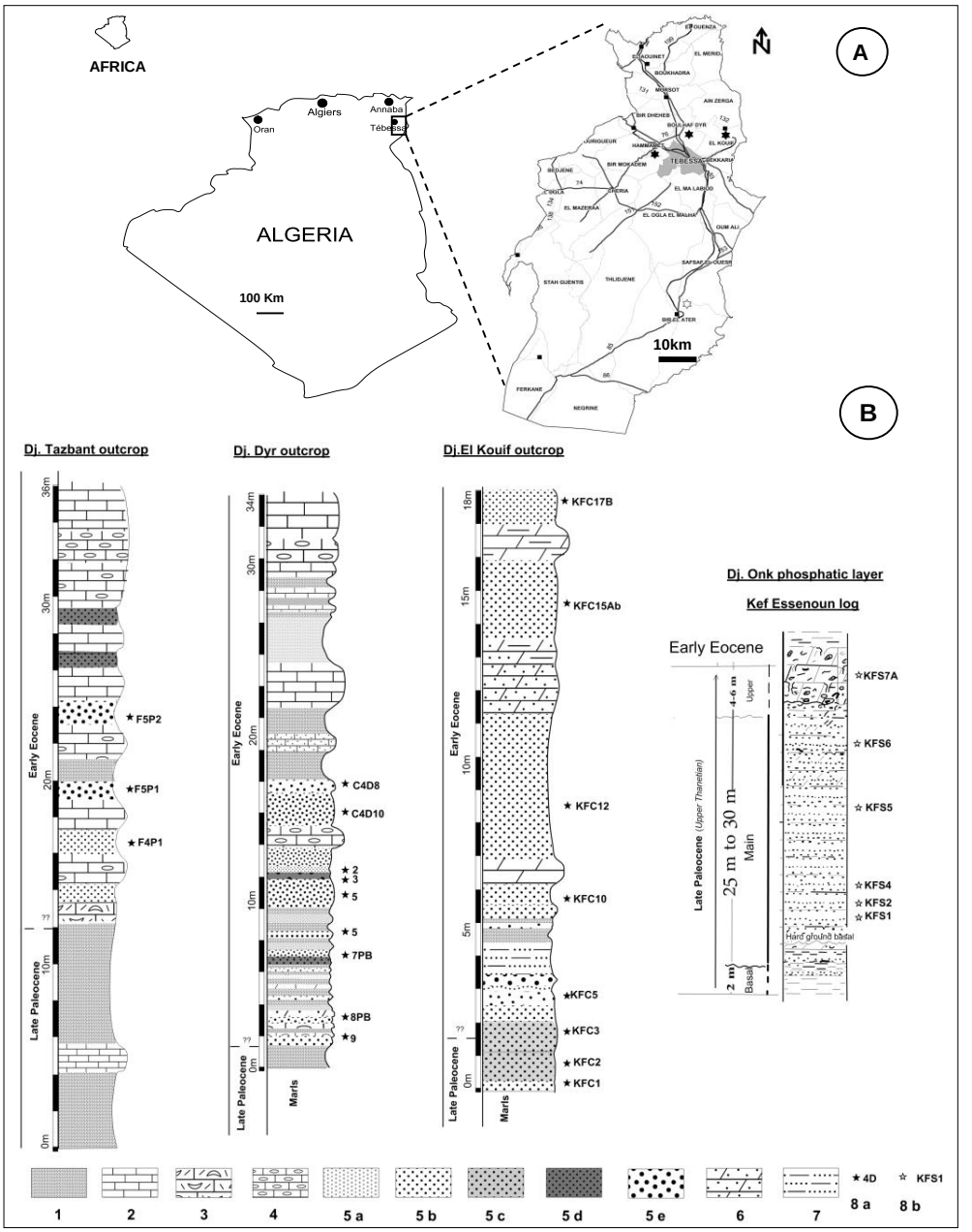

Fig. 2. (A) Location map of sampled deposits and showings in Tebessa region (northern localities: filled stars; southern locality: open stars). (B): Sampled lithological logs in the studied localities. 1 – marl; 2 – limestone; 3 – lumachelic limestone; 4 – cherty limestone; 5a – fine phosphorites; 5b – medium grained phosphorites; 5c – argillaceous phosphorites; 5d – Cherty dark phosphorites; 5e: coarse grained phosphorites; 6 – dolomitic phosphorites; 7 – Marly phosphorites; 8a – studied samples in northern localities; 8b – Studies samples in southern locality (Kef Essennoun) .

showings (3 samples) and one locality (Kef Essennoun, 6 samples) belongs to Djebel Onk district in the southern basin. Samples were taken from the different phosphorites layers as well as the host sedimentary rocks along cross-sections. The petrography was studied by the examination of thin sections under a microscope using both transmitted and reflected lights. Many samples were sieved using distilled water in order to study phosphatic particles. Pellets and coprolites were separated from their matrix; they show sizes ranging from 125µm to 250 µm

for pellets and from 250 µm to 500 µm for coprolites. X-ray diffraction (XRD) was used to determine the phosphorite mineralogy. XRD was performed using BRUCKER-AXS type D8 ADVANCE machine at Biskra University (Algeria). XRD characteristics are: radiation source Cu Kα with a wavelength λ of 1.540598 Å, acceleration voltage of 40 KV. The rare earth elements (REE) contents in whole-rocks were analyzed on untreated samples by Inductively Coupled Plasma Mass Spectrometry (ICP-MS) using a Thermofinnigan Element XR at Geosciences Montpellier (France). For each sample, about 50 mg of whole-rock powder was dissolved twice in a mixture of hydrofluoric acid (0.5 m HF) and nitric acid (1 ml HNO_3) on a hot plate at 110 °C for 48h. After dissolution, the solution was evaporated to dryness and diluted before analysis in HNO_3 2%.

4. Results

4.1. Mineralogy and petrography

The examination of thin sections shows that the main phosphorites are composed of particles with different shapes and sizes. Pellets are rounded to sub-rounded with grain size ranging from 80 µm to 250 µm, whereas coprolites have cylindrical to irregular forms with grain size ranging from 250 µm to 1 mm. Bioclasts, such as teeth and bones, are usually found in phosphorites The phosphorite particles are cemented by either argillaceous (soft phosphorites) or carbonaceous (hard phosphorites) matrix. Hand-picked phosphorite particles show mainly two colors in addition to different shapes and sizes. Indeed, pellets and coprolites are yellowish, milky to brown due to the content of organic matter and its oxidation degree. They sometimes present imprints of contact between grains which were acquired when the particles were still soft (Fig. 3. D; E; G). The XRD patterns performed on phosphorites of these localities show that Carbonate Fluor-apatite (CFA) is the main phosphatic mineral. Calcite, dolomite and quartz were found and represent the matrix of phosphorite grains (Fig. 3. F).

4.2. Rare earth elements (REE) abundances

The Dj. El Kouif phosphorites (Northern basin) show ∑REE contents ranging from 163.68 ppm to 472 ppm (average = 343.55 ppm). The Dj. Dyr and Tazbant showings (Northern basin) show a range of ∑REE from 125.45 ppm to 293.36 ppm (average = 213.59 ppm). The southern basin, represented by Kef Essennoun deposit, displays higher ∑REE contents (up to 906.39 ppm; average =623.01 ppm) compared to those of the northern basin. High REE contents are also reported in Tunisian, Egyptian, Jordanian and Iraqi phosphorites e.g. [8-10, 37-39]. It is worth noting that the ∑REE in the southern basin are enriched compared those of the Gafsa – Metlaoui basin (Table 1 to 3).

Table 1. Descriptive statistics of REE (ppm) in whole rock - Dj. El Kouif phosphorites belongs to the northern basin.

Element	Nb. Samples	Min.	Max.	Average	Variance	Standard Dev.
La	8.00	58.19	150.90	103.05	783.67	27.99
Ce	8.00	23.96	123.75	71.45	1294.95	35.99
Pr	8.00	7.01	22.17	15.82	30.28	5.50
Nd	8.00	31.10	96.33	69.29	555.41	23.57
Sm	8.00	5.85	18.29	13.15	20.99	4.58
Eu	8.00	1.57	5.02	3.51	1.45	1.20
Gd	8.00	8.87	26.10	17.23	28.03	5.29
Tb	8.00	1.23	3.70	2.45	0.57	0.75
Dy	8.00	9.06	27.03	17.35	26.80	5.18
Ho	8.00	2.23	6.42	4.01	1.36	1.17
Er	8.00	7.17	20.46	12.63	13.29	3.65
Tm	8.00	0.98	2.86	1.75	0.26	0.51
Yb	8.00	5.41	16.20	9.91	8.51	2.92
Lu	8.00	1.08	3.23	1.94	0.33	0.58
∑REE	8.00	163.68	472.44	343.55	12018.33	109.63
∑LREE (La To Eu)	8.00	127.67	392.77	276.28	8575.51	92.60
∑HREE (Gd to Lu)	8.00	36.01	106.00	67.27	391.32	19.78

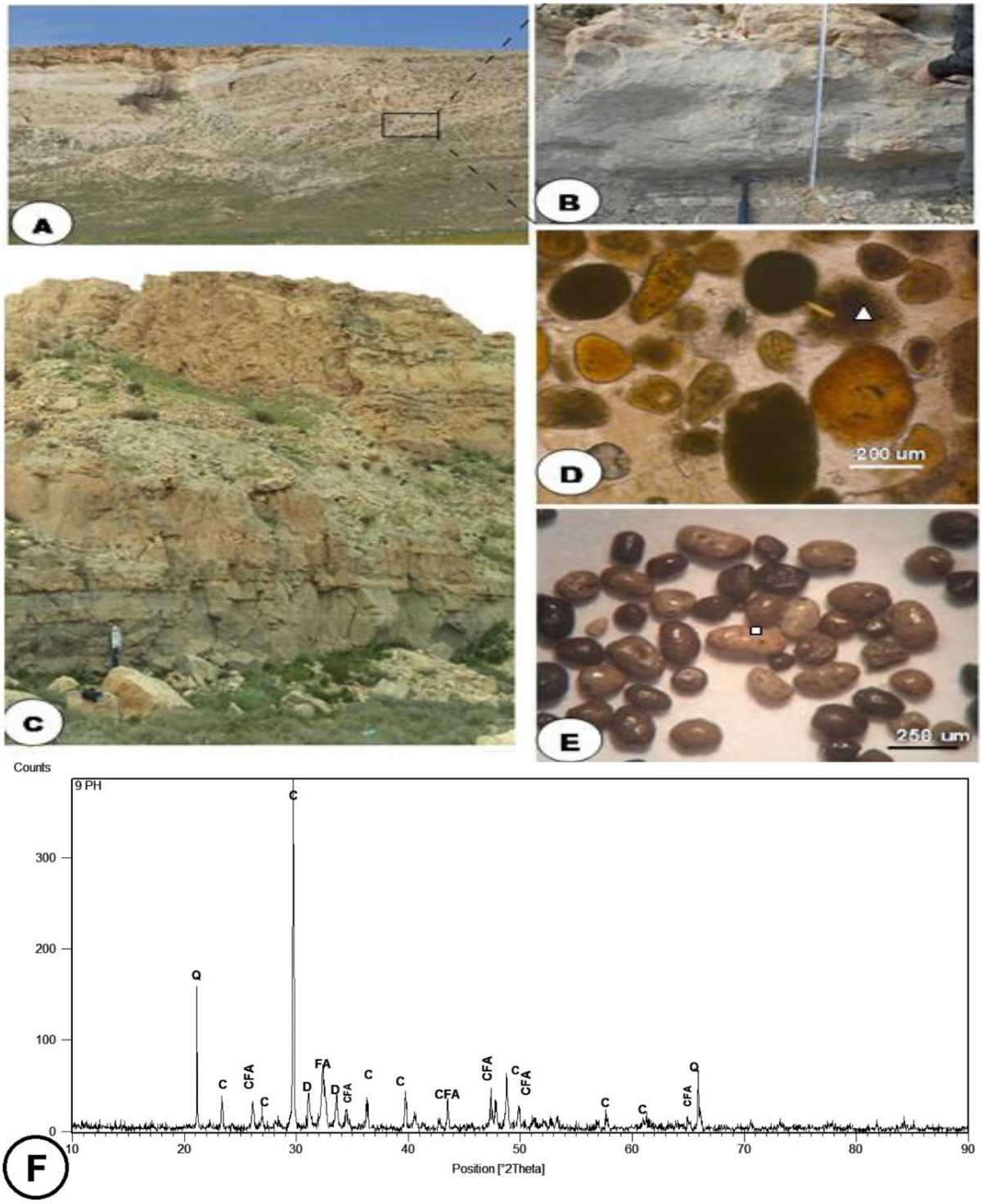
A
B
C
D
200 um
E
250 um
F
Counts
9 PH
Position [°2Theta]
Q
C
CFA
FA
D

Fig. 3. (A) Photograph of Djebel Dyr outcrop (northern phosphorite basin of Tebessa). (B) Main phosphorite layer at Dj. Dyr showing fine phosphorites with marly cement. (C) Photograph of Dj. El Kouif outcrop showing many phosphorites layers: clay-bearing, soft phosphorites at the bottom and hard phosphorites hosted by dolomite and limestone at the top. (D) Thin section of phosphorite sample from Dj. El Kouif (Paleocene – Eocene) showing phosphatic grains with different sizes and shapes (60 µm to 200 µm slightly rounded pellets; 200 µm to +500 µm cylindrical coprolithes; the white triangle show pellets as cement in the rock). (E) Pellets selection separated from their matrix. Pellets have different colors white – grey to brownish – dark. Pellets are borrowed due to contact with other grains (white square). (F) Example of X-ray diffraction pattern of phosphorite sample (in Dj. Dyr locality) showing the main phosphorite mineral (Carbonate Fluor-Apatite (CFA)), the exo-gangue represented by calcite (C), minor quartz (Q) and dolomite (D). (G) Coprolites from Dj. El Kouif phosphorite sample showing a cylindrical morphology, generally attributed to a fecal origin [40].

Table 2. Descriptive statistics of REE (ppm) in whole rock - Dj. Dyr (9 samples) and Tazbant showing (3 samples) phosphorites belong to the northern basin.

Element	Nb. Samples	Min.	Max.	Average	Variance	Standard Dev.
La	12.00	42.07	100.75	67.17	352.39	18.77
Ce	12.00	17.18	67.13	41.55	224.16	14.97
Pr	12.00	5.48	13.72	9.67	6.33	2.52
Nd	12.00	24.22	60.32	42.65	129.95	11.40
Sm	12.00	4.37	11.71	8.08	5.13	2.26
Eu	12.00	1.20	3.15	2.16	0.40	0.63
Gd	12.00	6.31	15.90	10.87	10.97	3.31
Tb	12.00	0.89	2.25	1.53	0.22	0.47
Dy	12.00	6.13	16.35	10.87	12.01	3.47
Ho	12.00	1.41	3.80	2.52	0.69	0.83
Er	12.00	4.33	12.24	7.98	7.27	2.70
Tm	12.00	0.59	1.72	1.10	0.14	0.37
Yb	12.00	3.31	9.88	6.23	4.51	2.12
Lu	12.00	0.63	1.96	1.22	0.18	0.42
∑REE	12.00	125.45	293.36	213.59	2981.02	54.60
∑LREE (La To Eu)	12.00	98.60	238.63	171.28	1804.71	42.48
∑HREE (Gd to Lu)	12.00	24.35	64.09	42.32	185.77	13.63

Table 3. Descriptive statistics of REE (ppm) in whole rock – Dj. Onk phosphorites belong to the southern basin.

Element	Nb. Samples	Min.	Max.	Average	Variance	Standard Dev.
La	6.00	64.61	199.20	144.23	1678.92	40.97
Ce	6.00	21.57	295.04	196.43	7167.12	84.66
Pr	6.00	7.53	47.87	32.65	153.99	12.41
Nd	6.00	33.28	207.25	138.66	2928.82	54.12
Sm	6.00	6.05	34.96	23.75	78.03	8.83
Eu	6.00	1.69	8.60	5.88	4.45	2.11
Gd	6.00	9.51	35.39	24.93	62.42	7.90
Tb	6.00	1.31	4.90	3.42	1.19	1.09
Dy	6.00	9.91	30.73	21.84	40.08	6.33
Ho	6.00	2.45	6.33	4.57	1.39	1.18
Er	6.00	7.93	18.24	13.42	9.97	3.16
Tm	6.00	1.09	2.43	1.78	0.17	0.41
Yb	6.00	6.24	13.07	9.67	4.46	2.11
Lu	6.00	1.24	2.39	1.79	0.13	0.36
∑REE	6.00	174.41	906.39	623.01	50580.90	224.90

∑LREE (La To Eu)	6.00	134.73	792.91	541.59	41061.24	202.64
∑HREE (Gd to Lu)	6.00	39.67	113.48	81.42	504.02	22.45

4.3. PAAS - Normalized REE

REE in investigated samples were normalized to Post Archean Australian shale (PAAS) [41]. In this paper, Cerium anomalies (Ce_{an}) were calculated using the method of Wright et al., 1987 [42]. Ce/Ce* denotes $3Ce_N/2(La_{N+}Nd_N)$. Ce_{An} as log Ce/Ce* ratio while $Pr/Pr^* = 2Pr_{N/}(Ce_{N+}Nd_{N)}$ [43]. PAAS-normalized REE patterns show enrichment in HREE in the northern localities. However, most samples in the southern locality are HREE depleted (Fig. 4). Patterns highlight a negative cerium anomaly in all phosphorites with different extents. We note that the sample from the upper sub-layer of phosphorites displays a pattern similar to the northern samples (Fig. 4 D.).

5. Discussions

5.1. Is Ce anomaly a real paleo redox indicator of phosphorite basins?

The negative cerium anomaly (Ce_{an}) indicates a deficiency in that element due the oxidation of Ce^{3+} to an insoluble state Ce^{4+} in oxidizing environments. Ce becomes fractionated and can make a cover on biological tests so that, it is partially removed from seawater [44]. Phosphorites with negative Ce_{an} indicate that they were formed under oxic conditions [3, 45-47]. Therefore, Ce_{an} can be used as a redox parameter providing the REE content is inherited from seawater and was not affected by post depositional alteration such as diagenesis and weathering which may mask or overprint the original signature. A diagram of $(La/Sm)_N$ versus $(La/Yb)_N$ [7] is used in this study to test the investigated samples against diagenesis effects (Fig. 5. A). It shows that all samples from the four localities (both northern and southern) have $(La/Sm)_N$ ratios ranging from 0.83 to 1.55, which is comparable to modern seawater (from 0.79 to 1.66 [7]). However, the $(La/Yb)_N$ ratios range from 0.67 to 1.18, which is higher than modern seawater (from 0.2 to 0.5 [7]). Some authors interpreted these high $(La/Yb)_N$ ratios by an adsorption of the REE onto apatite during early diagenesis [7]. The diagram of Bau and Dulski (1996) [43] is used to check the Ce_{an} strength. It consists of a projection of samples into a Pr/Pr* versus Ce/Ce* diagram (Fig. 5. B.). In this diagram, all samples are located in the IIIB area which indicates a real Ce_{an} and consequently this parameter is taken as a real paleoredox indicator. The calculated Ce_{An} highlight a significant difference between the northern and southern phosphorites. The Northern localities yield high Ce_{An} slightly variable between the three localities (Ce_{an} from -0.19 to -0.73, $\bar{x}$ = -0.49, σ = 0.17, n = 20). The Ce_{An} is increasing from western to eastern localities and indicates more oxidizing conditions towards Kessrine Island. In other word, we suggest that the depositional environment tend to be shallower in Dj. El Kouif deposit. We also note, that Ce_{An} increases relatively from bottom to upper layers. Samples from the southern locality show low Ce_{An} values compared to northern localities and it indicate a sub-oxic environment (Ce_{An} from -0.16 to -0.18, $\bar{x}$ = -0.176, σ = 0.01, n = 5), One sample from the upper sub-layer in this deposit shows a high Ce_{An} (-0.73), which indicates that redox conditions have changed to a more oxidizing environment.

5.2. Factorial discriminate analysis

Factorial discriminate analysis (FDA) is a multi-variate statistical method. Unlike principal component analysis, which summarizes the information focused on factors [48], FDA method aims at finding the sub-space of the original variable space that best separates the *m* classes by maximizing the inter-class variance regarding to the total variance [49-50]. This method is mainly based on several statistical hypotheses such as: prior probabilities, estimations of means and variances and equal dispersions [51]. FDA performed on samples issued from the four localities represents qualitative variables and their REE values are the explicative variables. Samples were projected on factorial axes, which show the variability cumulative of 94.98% (Fig. 5. C.). This highlights that samples are discriminated according to their REE signature and it shows an opposition between the northern and southern samples against F1 factor. Northern localities are slightly similar with nearby groups.

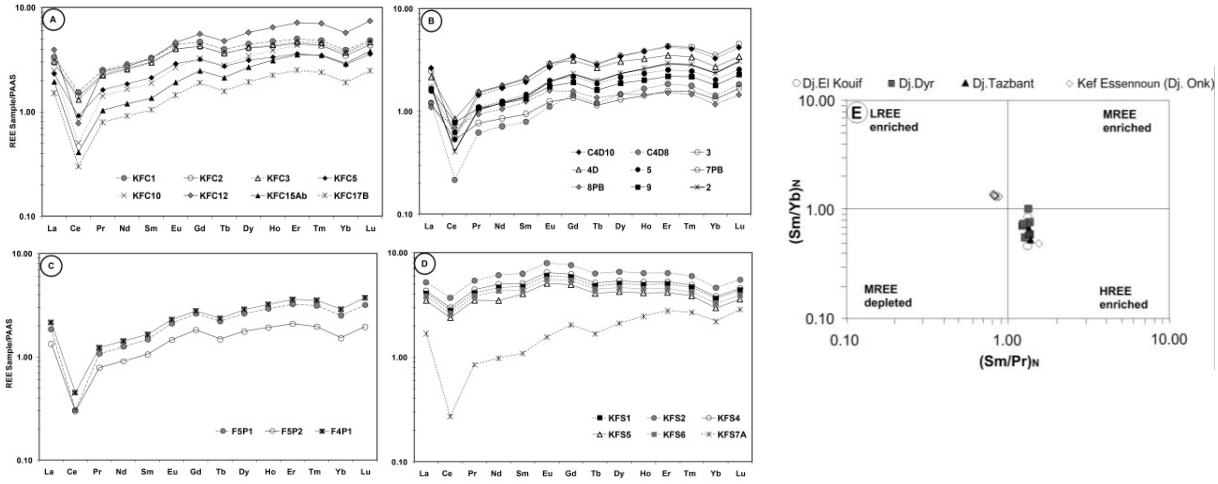

Fig. 4. PAAS - normalized REE patterns for investigated samples. Northern phosphorites show an enrichment in HREE: (A) Dj. El Kouif; (B) Dj. Dyr; (C) Dj. Tazbant showings. (D) Normalized REE patterns in southern locality (Kef Essenoun) show depletion in HREE except for one sample of the Upper sub-layer. (E) Binary Box plot of all samples show HREE enrichment in northern phosphorite samples.

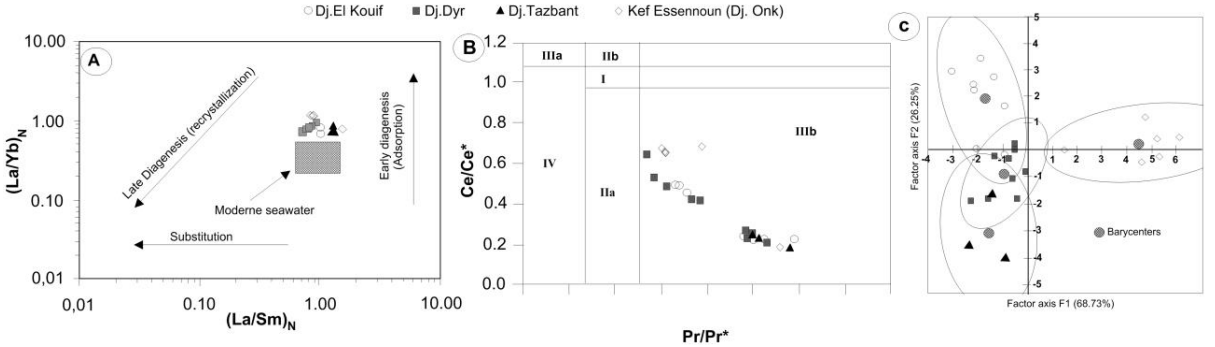

Fig. 5. (A) Binary plot of $(La/Sm)_N$ vs. $(La/Yb)_N$ ratios of studied samples reported in the diagram of Reynard et al. (1999) [7]. Samples show $(La/Sm)_N$ ratios similar to modern seawater, while their $(La/Yb)_N$ is higher indicating an early diagenetic process. (B) The Ce/Ce* vs. Pr/Pr* diagram [43]. Field I: no anomaly; Field IIa: positive La anomaly causes apparent negative Ce anomaly; Field IIb: negative La anomaly causes apparent positive Ce anomaly; Field IIIa: real positive Ce anomaly; Field IIIb: real negative Ce anomaly; Field IV: positive La anomaly disguises positive Ce anomaly. All samples show real negative Ce anomalies. (C) Scatter plot (F1 vs. F2) of studied samples from FDA analysis showing discriminate groups of phosphorites according to their location. The majority of Kef Essennoun (Djebel Onk) samples are grouped, except one sample from the upper sub-layer, which exhibits a similarity with northern phosphorites.

6. Conclusion

This study presents the preliminary results of REE analyses on Algerian phosphorites, located in the northeastern part of Algeria. During the course of this study, four (4) localities were investigated in the Tébessa region. These phosphorites are hosted in marine sedimentary formations of Late Paleocene to Early Eocene age. The REE analyses show a significant difference between the northern to southern phosphorites. PASS-normalized REE patterns indicate that the northern phosphorites are enriched in HREE while the majority of southern samples are HREE depleted. This study highlights that all phosphorites, while affected by early diagenetic processes, preserved the original signature inherited from paleoseawater. Cerium anomaly is used as a redox indicator. These phosphorites display real negative Ce anomalies although variable in extent. Therefore depositional environments were different in their redox conditions. The northern phosphorites show more pronounced negative Ce anomalies, which substantiates more oxigenated conditions. We suggest that the northern basin was connected to an open sea similarly to the Sra Ouartan basin in northern Tunisia [10]. Southern phosphorites show less pronounced negative cerium

anomalies, which indicate a sub-oxic environment characterized by a restricted water exchanges. These results are confirmed by factorial discriminate analysis.

References

[1] Altschuler, Z.S., Berman, S., Cuttitta, F., Rare earths in phosphorites-geochemistry and potential recovery, Geol. Survey Res., (1967), pp. 1–9.
[2] McArthur, J.M., Benmore, R.A., Bremner, J.M., Carbon and oxygen isotopic composition of structural carbonate in sedimentary francolite, J. Geol. Soc. (Lond.) 137 (1980) 669 – 673.
[3] J.M. McArthur, J.N. Walsh, Rare-earth geochemistry of phosphorites, Chemical Geology, 47 (1984) pp. 191–220.
[4] Elderfield, H., Sholkovitz, E.R., Rare earth elements in the pore waters of reducing near shore sediments, Earth Planet, Sci. Lett., 82 (1987), 280–288.
[5] Bau, M., Dulski, P., Distribution of yttrium and rare-earth elements in the Penge and Kuruman iron-formations, Transvaal Supergroup. Precambrian Res.79 (1996) pp. 37-55.
[6] Alibo, D. S. and Nozaki, Y. Rare earth elements in seawater: Particle association, shale-normalization and Ce oxidation, Geochim. Cosmochim. Acta 63 (1999) 363–372.
[7] Reynard, B., Lécuyer, C., Grandjean, P., Crystal-chemical controls on rare earth element concentrations in fossil biogenic apatites and implications for paleoenviro- mental reconstructions. Chem. Geol. 155, (1999), 233–241.
[8] Ismael, I.S, Rare earth elements in Egyptian phosphorites, Chinese journal of geochemistry, Jan. 2002, Vol. 21, Issue 1 (2002) pp 19-28.
[9] Ouanis, A., Kocsis, L., Chaabani, F., Pfeifer, H.R., Rare earth elements and stable isotope geochemistry (^{13}C and ^{18}O) of phosphorite deposits in the Gafsa Basin, Tunisia. Palaeogeogr. Palaeoclimatol. Palaeoecol, 268 (2008) 1-18.
[10] Garnit, H., Bouhlel, S., Barca, D. and Chtara, C., Application of LA-ICP-MS to sedimentary phosphatic particles from Tunisian phosphorite deposits: Insights from trace elements and REE into paleo-depositional environments, Chemie Erde-Geochemistry, Vol. 72, Issus 2, June 2012, pp. 127–139.
[11] Notholt, A.J.G., Economic phosphatic sediments: mode of occurrence and stratigraphical distribution. J. Geol. Soc. 137, (1980), pp. 793-805.
[12] Notholt, A.J.G., Sheldon, R.P., Davidson, D.F., Phosphate deposits of the world, Vol. 2, Cambridge Univ. Press, 1989, 566 pp.
[13] Sheldon, R.P., Association of phosphatic and siliceous marine sedimentary deposits. In: Hein, J.R. (Ed.), Siliceous sedimentary rock-hosted ores and petroleum, Van Norstrand Reinhold Co, New York, 1987, pp. 58-80.
[14] Sassi, A. B., Zaïer, A., Joron, J. L., & Treuil, M. (2005). Rare earth elements distribution of Tertiary phosphorites in Tunisia. In Mineral Deposit Res.: Meeting the Global Challenge (pp. 1061-1064). Springer Berlin Heidelberg.
[15] Lucas, J., Prevot-Lucas, L., Tethyan phosphates and bioproductites. In: Nairn, A.E., et al. (Eds.), the ocean basins and margins, The Tethys Ocean, vol. 8. Plenum Press (1995) pp. 367-391.
[16] Sassi, S., La sédimentation phosphatée au paléocène dans le sud et le centre ouest de la Tunisie. Thèse Doct. ès-Sci. Univ. Paris (1974).
[17] Burollet, P.F et Oudin, J.L., Paléocène et Eocène en Tunisie – pétrole et phosphate – in Géologie comparée des gisements de phosphate et de pétrole, Mém. BRGM n° 116 (1980).
[18] Fourine, D., Phosphates et pétrole en Tunisie, Mém. BRGM N.04 (1980), pp. 30-34.
[19] Winnock, E., Les dépôts de l'Eocène au Nord de l'Afrique: aperçu paléogéographique de l'ensemble, Géologie comparée des gisements de phosphates et de pétrole. Colloque International, Orléans, 6-7 Novembre 1979. BRGM 24, 1980, 219—243.
[20] Chaabani, F., Dynamique de la partie orientale du bassin de Gafsa au Crétacé et au Paléogène: Etude minéralogique et géochimique de la série phosphatée Eocène, Tunisie méridionale. Thèse Doct. Etat, Univ. Tunis II, Tunisie (1995).
[21] Zaïer, A., Beji-Sassi, A., Sassi, S., Moody, R.T.J., Basin evolution and deposition during the Early Paleocene in Tunisia. In: Macgregor, D.S., Moody, R.T.J., Clark- Lowes, D.D. (Eds.), Petroleum Geology of North Africa. Geol. Soc. London Spec. Publ., v. 132, 1998, pp. 375–393.
[22] Dubourdieu, G., Étude géologique de la région de l'Ouenza (confins algéro-tunisiens), Pub. Ser. de la carte géol. de l'Algérie, Nouvelle Série, (1956) pp. 1–659.
[23] Durozoy, G., Bouillon, M., Carte géologique de l'Algérie au 1/50000, Feuille 206-Tébessa. Service de la carte géol. de l'Algérie (1956).
[24] Blès, J.L., Fleury, J.J., Carte géologique de l'Algérie au 1/50000. Feuille 178 - Morsott, Service de la carte géologique de l'Algérie (1970).
[25] Rouvier, H., Géologie de l'Extrême Nord - tunisien: Tectonique et paléogéographies superposées à l'extrémité orientale de la chaîne nord-maghrébine. Thèse d'Etat, Paris VI, 703 (1977) pp.
[26] Perthuisot, V., Dynamique et pétrogenèse des extrusions triasiques en Tunisie septentrionale. Travaux du lab. de geol. de I'E.N.S., Paris, N°21 (1978), 312 pages.
[27] Vila, J.M., La chaîne alpine d'Algérie orientale et des confins algéro-tunisiens. Université Paris VI (1980) 665 p.
[28] Zaïer, A., Evolution tectno-sédimentaire du bassin phosphate du centre-ouest de la Tunisie minéralogie, pétrographie, géochimie et genèse des phosphorites. Thèse Doct. Es-Sci. Univ. Tunis II (1999).
[29] Kowalski, W.M., Hamimed, M., Pharisat, A., Les étapes d'effondrement des grabens dans les confins algéro-tunisiens. Bull. Serv. Geol. Algérie, V.13, n°2, 2002, p.131-152.
[30] Chaabani, F., Dynamique de la partie orientale du bassin de Gafsa au Crétacé et au Paléogène: Etude minéralogique et géochimique de la série phosphatée Eocène, Tunisie méridionale. Thèse Doct. Etat, Univ. Tunis II, Tunisie (1995).
[31] Visse, L., Genesis of the southeasterly Algerian–Tunisian phosphatic deposits, XIX International Geological Congress., set 1, no. 27, Algiers, Algeria, (1952), pp. 60.
[32] Kassatkine, Y., Yahyaoui. A., Chatilov, S., The works of prospecting and assessment on phosphate executed in 1976–1978 in the mining district of Djebel Onk. SO.NA.RE.M Internal report, vol. 2, Alegria, 1980, pp 140
[33] Ranchin, G., The sedimentary phosphates of lime in Djebel Onk's region (Algeria), S.E.R.M. Paris, France, 1963, pp 85.
[34] Chabbou-Moustafai, S., Etude de la série phosphatée tertiaire du Djebel Onk (Algérie): stratigraphie, pétrographie, minéralogie et géochimie. Thèse Doct. ès-Sci. Univ. Aix-Marseille, France (1987).
[35] Cielensky, S., Benchernine, N., Watkowski, T., Works of prospecting and assessment of phosphates in the region of Bir El Ater. Internal report, EREM (Entreprise de Recherche et d'Exploration Minière), vol. 2, Algeria, 1988, pp. 103.
[36] Prian, G.P. and Cortiel Ph., Development study of phosphate deposit of Djebel Onk (Algeria). Geological expertise report, B.R.G.M

(Bureau de Recherches Géologiques et Minières, Orléans) France, 1993, pp. 288.
[37] Abed, A.M. and Abu Murry, O.S., Rare earth elements geochemistry of the Jordanian Upper Cretaceous phosphorites. Arab. Gulf J. Sci. Res., 15.1 (1997) 41-61.
[38] Abu Murry, O.S., Distribution of rare earth elements in Jordanian phosphorites, M. Sc. Thesis, University of Jordan, Amman, Jordan (1993).
[39] Tlig, S., Sassi, A., Belayouni, H., & Michel, D. (1987). Distribution de l'uranium, du thorium, du zirconium, du hafnium et des terres rares (TR) dans des grains de phosphates sédimentaires. Chem. Geol., 62(3), 209-221.
[40] Ben Hassen, A., Trichet, J., Disnar, J.R., Pétrographie et géochimie comparées des pellets phosphatés et de leur gangue dans le gisement phosphaté de Ras-Draaa (Tunisie). Implications sur la génèse des pellets phosphatés. Swiss J. Geosciences, 103 (3), 2010, pp. 457-473.
[41] McLennan, S.M., Rare earth elements in sedimentary rocks: Influence of provenance and sedimentary processes. In: Lipin, B.R., McKay, G.A. (Eds.), Geochemistry and mineralogy of rare earth elements. Min. Soc. Am. Rev. Miner. 21, (1989) 169-200.
[42] Wright, J., Schrader, H., Holser, W.T., 1987. Paleoredox variations in ancient oceans recorded by rare earth elements in fossil apatite. Geochim. Cosmochim. Acta. 51, 631–644.
[43] Bau, M., Dulski, P., Distribution of Yttrium and rare earth elements in the Penge and kuruman iron-formations, Transvaal supergroup. Precambrian Res. 79, 1996, pp. 37–55.
[44] Sholkovitz, E., Landing, W.M., Lewis, B.L., Ocean particle chemistry: the fractionation of the rare earth elements between suspended particles and seawater. Geochim. Cosmochim. Acta 58, (1994) pp. 1567–1580.
[45] Goldberg, E.D., Chemistry in the Ocean. In: Sears, M. (eds), Oceangraphy, Am. Associa. Adv. Sci. 67 (1961) pp. 583-597.
[46] Piper, D.Z., Rare earth elements in sedimentary cycle, Chem. Geol., 14 (1974) 285-304.
[47] Elderfield, H. and Greeves, M.J., The rare earth elements in seawater, Nature, 297 (1982), pp. 214-219.
[48] Bakalowicz, M., Contribution de la géochimie des eaux à la connaissance de l'aquifère karstique et de la karstification. Doct. Thesis, Paris VI, 1979, p. 269.
[49] Fisher, R., The use of multiple measurements in taxonomic problems. Ann. Eugenics 7, 1936, 179–188.
[50] Romeder, J.M., Méthodes et programmes d'analyse discriminante, Dunod, Paris, France (1973).
[51] Williams, B.K., Some observations on the use of discriminate analysis in ecology, Ecology 64 (5), (1983)1283–1291.